Journal of Biomedical Optics

BiomedicalOptics.SPIEDigitalLibrary.org

Differentiating cancerous tissues from noncancerous tissues using single-fiber reflectance spectroscopy with different fiber diameters

Aslinur Sircan-Kuçuksayan
Tuba Denkceken
Murat Canpolat

SPIE.

Journal of Biomedical Optics 20(11), 115007 (November 2015)

Differentiating cancerous tissues from noncancerous tissues using single-fiber reflectance spectroscopy with different fiber diameters

Aslinur Sircan-Kuçuksayan,[a] Tuba Denkceken,[b] and Murat Canpolat[a,*]
[a]Akdeniz University, Department of Biophysics, Biomedical Optics Research Unit, Faculty of Medicine, Dumlupınar Bulvari, Antalya 07058, Turkey
[b]Sanko University, Department of Biophysics, Faculty of Medicine, Incilipinar Mah. Gazi Muhtar Paşa Bulvari, No. 36, Gaziantep 27090, Turkey

Abstract. Elastic light-scattering spectra acquired with single-fiber optical probes with diameters of 100, 200, 400, 600, 800, 1000, 1200, and 1500 μm were used to differentiate cancerous from noncancerous prostate tissues. The spectra were acquired *ex vivo* on 24 excised prostate tissue samples collected from four patients. For each probe, the spectra and histopathology results were compared in order to investigate the correlation between the core diameters of the single-fiber optical probe and successful differentiation between cancerous and noncancerous prostate tissues. The spectra acquired using probes with a fiber core diameter of 400 μm or smaller successfully differentiated cancerous from noncancerous prostate tissues. Next, the spectra were acquired from monosized polystyrene microspheres with a diameter of 5.00 ± 0.01 μm to investigate the correlation between the core diameters of the probes and the Mie oscillations on the spectra. Monte Carlo simulations of the light distribution of the tissue phantoms were run to interrogate whether the light detected by the probes with different fiber core diameters was in the ballistic or diffusive regime. If the single-fiber optical probes detect light in the ballistic regime, the spectra can be used to differentiate between cancerous and noncancerous tissues. [DOI: 10.1117/1.JBO.20.11.115007]

Keywords: single fiber; cancerous tissue; light scattering; polystyrene; reflectance; spectroscopy.

Paper 150261RRRR received Apr. 20, 2015; accepted for publication Oct. 21, 2015; published online Nov. 23, 2015.

1 Introduction

Backreflection spectroscopy is a new modality to estimate optical properties of pathological tissues for diagnostic purposes.[1–4] One of the spectroscopic means for the detection of cancerous tissue is elastic light single-scattering spectroscopy (ELSSS).[5–8] It has been shown that single-fiber optical probes detect single-scattered photons from a turbid medium rather than multiple scattered photons, and thus provide information about the size of scatters.[9,10] In general, the spectrum of single-scattered photons from turbid media changes with the size and shape of the scatters and the ratio of the refraction index of scatters to that of the surrounding medium. Light scatters from cell membranes, nuclei, and other organelles in the tissue.[11] It has been shown that spectra acquired using a single-fiber optical probe with a diameter of 100 μm from noncancerous and cancerous tissues linearly increase and decrease, respectively, within the wavelength range of 450 to 700 nm.[12–16] Therefore, the sign of the spectral slope can be used to differentiate cancerous tissue from noncancerous, as it is negative for the former and positive for the latter. However, it has not been investigated what the diameter range of the single-fiber optical probe should be to be able to differentiate between cancerous and noncancerous tissues.

2 Materials and Methods

2.1 *Single-Fiber Reflectance Spectroscopy*

The single-fiber reflectance spectroscopy system consisted of a spectrometer (USB2000 with OOIBase32TM Platinum Spectrometer Operating Software, Ocean Optics, Tampa, Florida), a tungsten-halogen white-light source (HD2000, Ocean Optics), and single-fiber optical probes with fiber diameters of 100, 200, 400, 600, 800, 1000, 1200, and 1500 μm. The single-fiber optical probes with a diameter of 100 and 200 μm were 1×2 fused fiber optical couplers with a split ratio of 50% (Fiber Optic Network Technology, Co., Surrey, British Columbia). All other single-fiber optical probes were built in-house by end-coupling two fibers onto the face of a fiber with a larger diameter with a sub miniature A (SMA) connector; for example, two 200-μm-diameter fibers facing toward a larger one in an SMA barrel connector. The single-fiber optical probes were used for both delivery and detection of white light to and from tissue, as illustrated in Fig. 1. One distal end of the probe was connected to a white-light source (Ocean Optics, LS1), while the other end was connected to a spectrometer (Ocean Optics, USB2000).

The spectra were obtained in the wavelength range of 400 to 850 nm. The parts of the spectrum that fell below 450 and above 750 nm were not included in the data processing because of high

*Address all correspondence to: Murat Canpolat, E-mail: canpolat@akdeniz.edu.tr

1083-3668/2015/$25.00

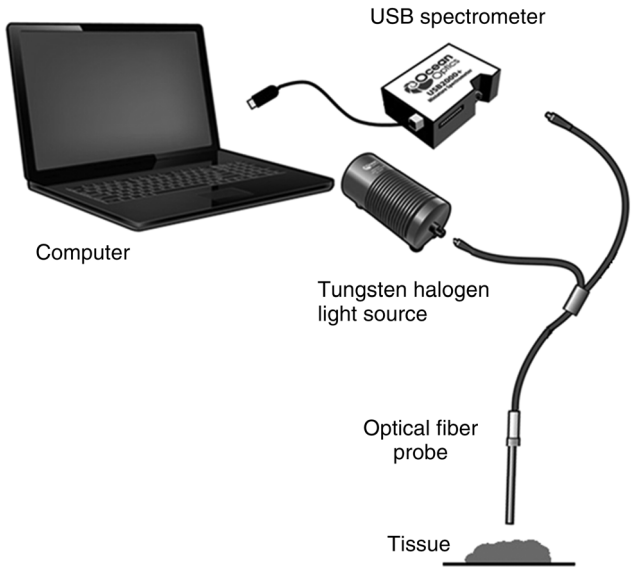

Fig. 1 The single-fiber reflectance spectroscopy system consists of a tungsten-halogen light source, an optical fiber probe, a spectrometer, and a laptop.

noise levels. Therefore, the range of the fit was 450 to 750 nm. The corrected spectrum $R(\lambda)$ is

$$R(\lambda) = \frac{R_s(\lambda) - R_{bg}(\lambda)}{R_c(\lambda) - R_{bg}(\lambda)}, \quad (1)$$

where $R_s(\lambda)$ is a spectrum of scattering medium, $R_c(\lambda)$ is a spectrum of Spectralon (Labsphere, Inc., North Sutton, New Hampshire) in water, and $R_{bg}(\lambda)$ is a background spectrum taken from pure water in a black container. All the spectra are acquired and calibrated as described in detail elsewhere.[9] The amount of light delivered to the tissues changes with the diameter of the optical fiber probe. In order to eliminate differences in the power of the light delivered by the optical fiber probes with different diameters, the areas under the spectra in the wavelength range of 450 to 750 nm were normalized.

2.2 *Cancerous and Noncancerous Prostate Tissues*

The clinical study was conducted at Akdeniz University Hospital with the approval of the Akdeniz University Institutional Review Board. Four patients undergoing open radical prostatectomy at Akdeniz University Urology Department were recruited for the collection of cancerous and noncancerous prostate tissues. Just after the surgery, the prostate tissues were carried from the surgery to the pathology room in the serum physiological solution. Prostate tissues were put in pathology cassettes and were classified by gross visual examination as cancerous or noncancerous and confirmed by histopathological examination. Eight ELSSS measurements were performed per tissue within 15 to 20 min, on a surface area of 3 to 4 mm^2 using optical fiber probes with different diameters. During the measurements, serum physiological solution was dripped on the tissue samples to prevent them from drying. The spectra obtained from different sites of the same tissue were similar to each other, indicating that there was no significant variation in optical properties for different sites within one tissue.

The spectra were acquired from three cancerous and three noncancerous prostate tissues of each patient. In total, spectra were acquired from 12 noncancerous and 12 cancerous *ex vivo* tissues of four patients. The different single-fiber optical probes were used each time in the same order (probe with fiber diameter of 100, 200, 400, 600, 800, 1000, 1200, and 1500 μm). The probe with a diameter of 100 μm was used at both the beginning and the end of the data acquisition in order to investigate variation of the tissue spectra over time during the course of the *ex vivo* measurements. No changes were observed between the spectra in the beginning and at the end of the data acquisition using the 100-μm-diameter fiber. After the spectroscopic examinations, all tissues were sent to the histopathology room.

2.3 *Tissue Phantoms*

The tissue phantoms used in the experiments consisted of 1.25% aqueous suspensions of monodisperse polystyrene microspheres with a diameter of 5 μm (Thermo Scientific, Waltham, Massachusetts). Reduced scattering coefficients of different tissue types vary in the ranges of 1.2 to 40 cm^{-1}.[17] We have chosen the reduced scattering coefficient of the tissue phantom as 10.5 cm^{-1} at a wavelength of 633 nm. Mie theory was used to calculate the reduced scattering coefficients of the tissue phantoms using a value of 1.58 for the scatterer and 1.33 for the water index of refraction, respectively.[9] After calibration, the tips of the probes with different diameters were inserted in the tissue phantoms and spectra were acquired. Mie oscillations were seen on all the spectra; however, the amplitude of the oscillations decreased with an increased core diameter of the single-fiber optical probes.

2.4 *Monte Carlo Simulations*

Monte Carlo (MC) simulations of light distribution in the tissue phantom were run for the single-fiber optical probes[9] with core diameters of 100, 200, 400, 600, 800, 1000, 1200, and 1500 μm. The wavelength range was between 500 and 700 nm in the simulations and for every second wavelength, 500,000 photons were sent. The reduced scattering coefficient and anisotropy coefficient were 10.5 cm^{-1} and 0.8, respectively, at a wavelength of 633 nm. Background absorption in the simulation was zero, since absorption of light in the tissue phantoms was negligible. For each MC run, the number of scattering events and optical path length of the detected photons were calculated.

3 Results

All the spectra acquired from the cancerous and noncancerous prostate tissues using the single-fiber optical probes were corrected using Eq. (1). A correlation between the spectral measurements and the results of histopathology analysis was investigated. The spectra in Fig. 2 were acquired from noncancerous and cancerous prostate tissues using a probe with a fiber core diameter of 100 μm. The average nucleus area is larger for cancerous than noncancerous prostate tissues. The spectral slopes are positive for normal prostate tissue and negative for cancerous tissues, where spectral shapes are correlated with the average nucleus area. The average spectra of healthy and cancerous prostate tissues acquired by the probe with diameters of 100 and 1000 μm are displayed in Fig. 3. The spectral slopes of the spectra acquired using the probe with a diameter of

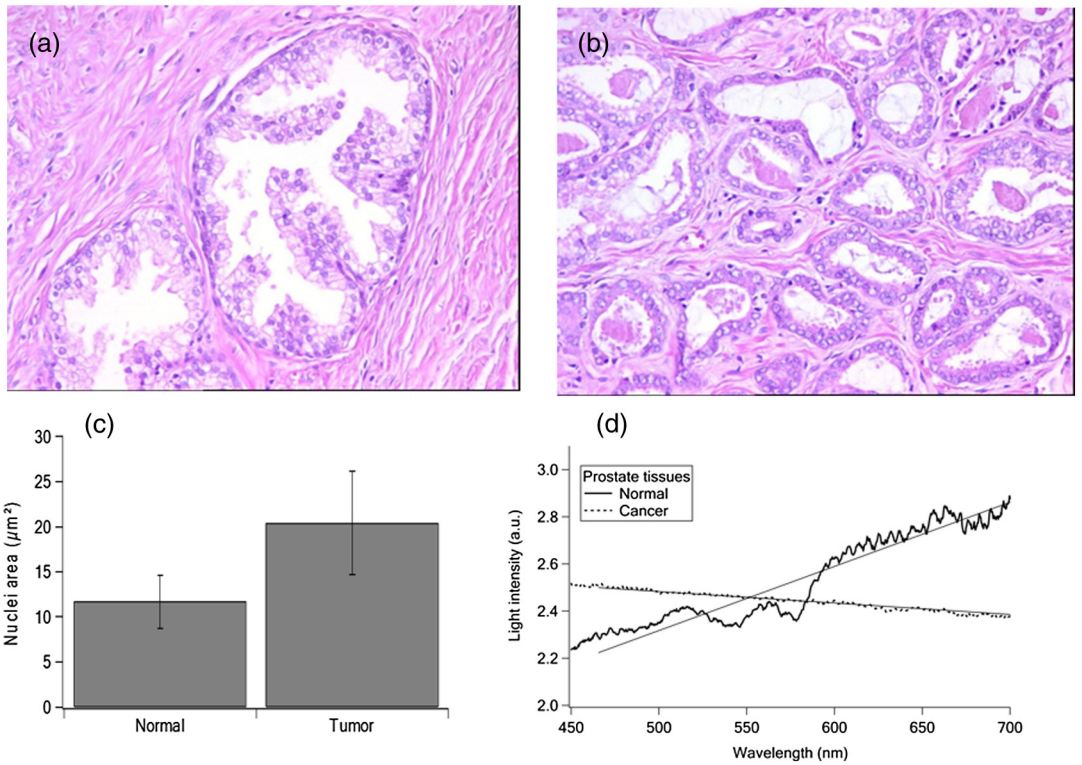

Fig. 2 (a) Histological appearance of normal prostate tissue, H&E 200× magnification. (b) Histological appearance of cancerous prostate tissue, H&E 200× magnification. (c) The average nuclear area is twice as large in cancerous than in normal prostate tissues. (d) Spectra acquired from noncancerous and cancerous prostate tissues using the single-fiber optical probe with a diameter of 100 μm.

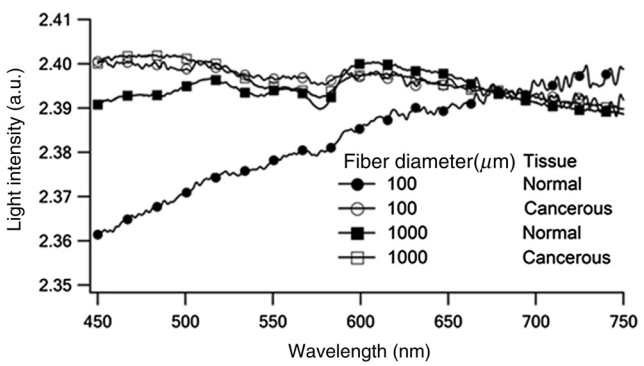

Fig. 3 Spectra acquired from prostate cancerous and noncancerous tissues using single-fiber optical probes with diameters of 100 and 1000 μm.

100 μm from the normal tissue are positive, and those of the cancerous tissue spectra are negative. The spectral slopes are negative for the spectra of both normal and cancerous tissues obtained using the 1000-μm-diameter probe (Fig. 3). The single-fiber optical probe with a diameter of 100 μm acquired different spectra from cancerous and noncancerous tissues, but the probe with a diameter of 1000 μm acquired similar spectra for both cancerous and noncancerous tissues.

Spectral slopes of the average spectra acquired from normal and cancerous prostate tissues using all the single-fiber optical probes are shown in Fig. 4. Spectral slopes of the spectra acquired from noncancerous tissue are shown in Fig. 4(a), while those of cancerous tissue are displayed in Fig. 4(b). The signs of the slopes of the spectra acquired by 100-, 200-, and 400-μm-diameter probes from noncancerous prostate tissues were positive and those from cancerous prostate tissues

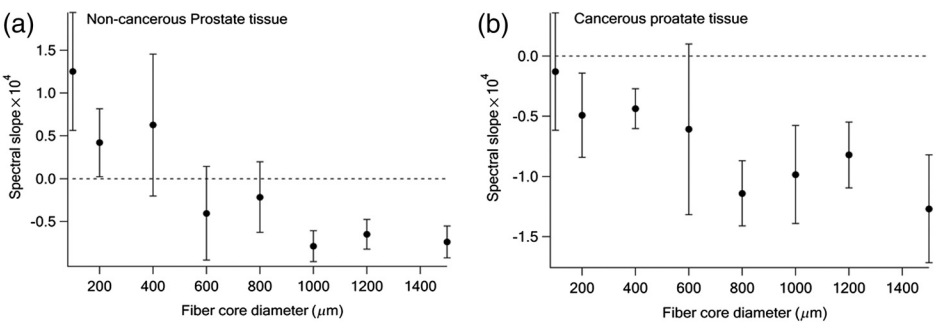

Fig. 4 (a) Spectral slopes of spectra acquired from noncancerous prostate tissues. (b) Spectral slopes of spectra acquired from cancerous prostate tissues.

Table 1 Spectral slopes of the spectra acquired from noncancerous and cancerous prostate tissues of four patients using the single-fiber optical probe with the core diameters in the range of 100 to 1500 μm.

Probe diameter (μm)	Patient 1		Patient 2		Patient 3		Patient 4		Average	
	Spectral slopes $\times 10^4$		Spectral slopes $\times 10^4$		Spectral slopes $\times 10^4$		Spectral slopes $\times 10^4$			
	Normal	Tumor	Normal	Tumor	Normal	Tumor	Normal	Tumor	Normal	Tumor
100	2.03 ± 0.01	−0.41 ± 0.01	0.78 ± 0.01	−0.52 ± 0.01	1.62 ± 0.02	−0.15 ± 0.02	0.58 ± 0.01	0.57 ± 0.01	1.25 ± 0.69	−0.13 ± 0.49
200	0.96 ± 0.01	0.02 ± 0.01	0.38 ± 0.02	−0.59 ± 0.03	0.32 ± 0.01	−0.74 ± 0.02	0.02 ± 0.02	−0.66 ± 0.02	0.42 ± 0.39	−0.49 ± 0.35
400	1.80 ± 0.04	0.05 ± 0.03	0.09 ± 0.01	0.01 ± 0.01	0.01 ± 0.01	−0.29 ± 0.03	0.61 ± 0.03	0.06 ± 0.02	0.63 ± 0.83	−0.04 ± 0.16
600	0.38 ± 0.01	0.21 ± 0.01	−0.75 ± 0.01	−0.48 ± 0.01	−0.79 ± 0.02	−1.52 ± 0.03	−0.45 ± 0.02	−0.64 ± 0.03	−0.45 ± 0.55	−0.61 ± 0.71
800	−0.04 ± 0.02	−1.22 ± 0.01	−0.42 ± 0.01	−1.48 ± 0.02	0.52 ± 0.01	−1.02 ± 0.02	−0.92 ± 0.01	−0.85 ± 0.01	−0.22 ± 0.61	−1.14 ± 0.27
1000	−0.95 ± 0.01	−0.79 ± 0.01	−0.91 ± 0.01	−0.57 ± 0.01	−0.55 ± 0.01	−1.51 ± 0.02	−0.74 ± 0.01	−1.07 ± 0.01	−0.79 ± 0.18	−0.98 ± 0.41
1200	−0.87 ± 0.01	−0.60 ± 0.01	−0.44 ± 0.01	−0.57 ± 0.01	−0.66 ± 0.01	−1.01 ± 0.02	−0.63 ± 0.01	−1.10 ± 0.01	−0.65 ± 0.17	−0.82 ± 0.27
1500	−0.94 ± 0.01	−1.34 ± 0.01	−0.48 ± 0.01	−0.74 ± 0.01	−0.76 ± 0.01	−1.83 ± 0.02	−0.78 ± 0.01	−1.17 ± 0.01	−0.74 ± 0.19	−1.27 ± 0.45

were negative. The spectral slopes of the spectra acquired using optical probes with a diameter larger than 400 μm were negative for both noncancerous and cancerous prostate tissues.

Based on the sign of the spectral slopes in Table 1, a sensitivity of 100% and a specificity of 58% can be obtained for the detection of cancerous prostate tissues, based on the combined results obtained using optical fibers with core diameters of 100, 200, and 400 μm. The sign of the spectral slopes is close to zero but not negative for the spectra acquired from cancerous prostate tissue for the fiber with a core diameter of 400 μm. If we do not take this into account, the sensitivity and specificity of the probes with a diameter of 100 and 200 μm are 100% and 75%, respectively.

4 Discussion

We show that the spectra acquired using single-fiber optical probes with a diameter of 400 μm or smaller may be used to differentiate cancerous tissue from noncancerous tissue. The spectra acquired using probes with a fiber core diameter larger than 400 μm cannot be used to differentiate between cancerous and noncancerous tissues based on the sign of the spectral slopes because it is negative for both tissue types.

In order to investigate the differences between the spectra acquired using the single-fiber optical probes with different diameters, we analyzed the spectra acquired from the tissue phantoms and those obtained by MC simulations. As seen in Fig. 5, the spectra of the tissue phantom acquired using 100- and 1000-μm fiber diameter probes are different from each other for both experiments and MC simulations. The amplitude of the Mie oscillations of the spectrum acquired using the probe with a fiber diameter of 100 μm is larger than the oscillation of the spectrum obtained by the probe with a 1000-μm fiber diameter.

The intensity of the detected light by a single-fiber optical probe with a larger fiber diameter is higher; therefore, the areas under the spectra in the wavelength range of 450 to 750 nm were normalized as shown in Fig. 5. The absolute amplitude (AA) of the Mie oscillations in Fig. 5 is defined as

$$\mathrm{AA} = \frac{I_{\max} - I_{\min}}{(I_{\max} + I_{\min})/2}. \tag{2}$$

AA is independent of the intensity of the detected light by the probe and only provides information about the amplitude of the

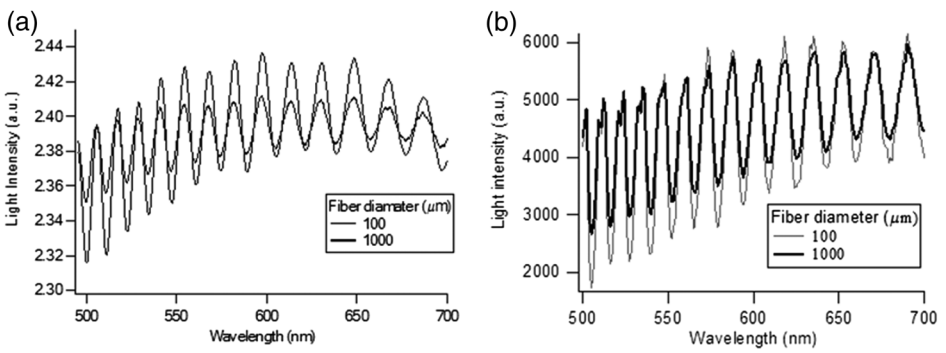

Fig. 5 (a) Spectra acquired from the tissue phantom with reduced scattering coefficient of 10.5 cm^{-1} using probes with fiber diameters of 100 and 1000 μm. (b) Spectra obtained from the Monte Carlo (MC) simulations for the same experiments. The area under the spectra in the wavelength range of 500 to 700 nm was normalized for visual presentation.

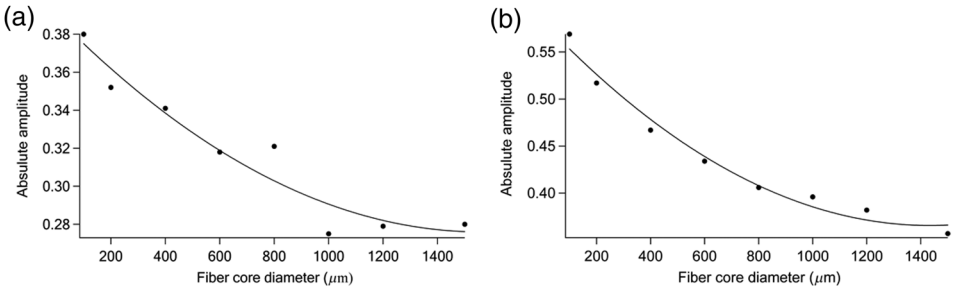

Fig. 6 Variation of the absolute amplitude (AA) of the oscillations on the spectra acquired using probes with a fiber diameter in the range of 100 to 1500 μm. The AA obtained from the (a) experiments, (b) MC simulations.

oscillations for the wavelengths between 500 and 700 nm. The AA decreases with increasing probe fiber diameter, as seen in Fig. 6, for both the experiments and the MC simulations. The variations of the amplitudes versus the fiber core diameters shown in Figs. 6(a) and 6(b) are similar to each other. Therefore, we may assume that microscopic parameters such as number of scattering events and path length of the detected photons by the single-fiber optical probe in the tissue phantoms experiments are the same as for the simulations.

The average reduced scattering coefficient, μ_s', over all wavelengths used in the MC simulation is 11.32 cm^{-1}, the average g value is 0.87, and the transport mean free path (TMFP) $(1/\mu_s')$ is 0.088 cm. The light enters the diffusive regime after $(1-g)^{-1}$ scattering events, which is 7.7 for the tissue phantom. If the photon propagation is less than one TMFP, photons are largely in the ballistic regime. When the travel distance is more than one TMPF, more scattering occurs and the light in a more diffusive regime.

MC simulation results reveal that the average number of scattering events and the optical path length of the detected photons increase linearly with the fiber core diameter (Fig. 7). The average path length of the photons detected by the probe with a diameter of 400 μm is 0.082 cm, which is smaller than the TMFP, and the average number of the scattering events is 7.42, which is smaller than the number of average scattering events (7.7) to be in the ballistic regime. Therefore, the single-fiber optical probes with a diameter of 400 μm detect the reflected light in a ballistic regime and the spectra change with size distribution of the scatters in the tissues. For the light detected by the 600-μm-diameter optical fiber, the number of average scattering events is 10 and the average path length of the detected photons is 0.108 cm. Since these values are larger than the TMFP and average number of the scattering events (7.7) to be in the ballistic regime, most of the photons detected by this probe are in the diffusive regime. Therefore, spectra obtained by the probe with a diameter of 600 μm or larger do not differentiate between the cancerous and noncancerous tissues.

In the ballistic scattering regime, spectra of the detected photons depend on the phase function of the scattered light for a small source-to-detector distance.[18] In the present study, it has been shown that probes with a diameter of 400 μm or smaller detect photons in the ballistic scattering regime. Therefore, spectra of single-fiber optical probes with an optical fiber diameter smaller or equal than 400 μm are sensitive to the size of the scatters. Light scatters in a medium because of heterogeneity in the index of refraction. In tissue, light scattering takes place at cell membranes due to the greater refraction index of membranes compared to that of extracellular liquid. Light also scatters inside the cells at membranes of nuclei, mitochondria, and other organelles because of the differences in the refraction index of the membrane (1.48) and cytoplasm (1.38).[11] Phase function of the scattered light depends on the size distribution of the scatters, the relative index of refraction of scatters to the surrounding medium, and the wavelength of the light. The phase function of the cancerous cells is different than that of normal cells due to the presence of enlarged nuclei in cancerous cells.[19] Therefore, in the ballistic scattering regime, spectra of the single-fiber optical probe with a diameter equal to or smaller than 400 μm are different for normal and cancerous tissues. It has been shown that the wavelength dependency of the optical properties of normal and cancerous prostate tissue is

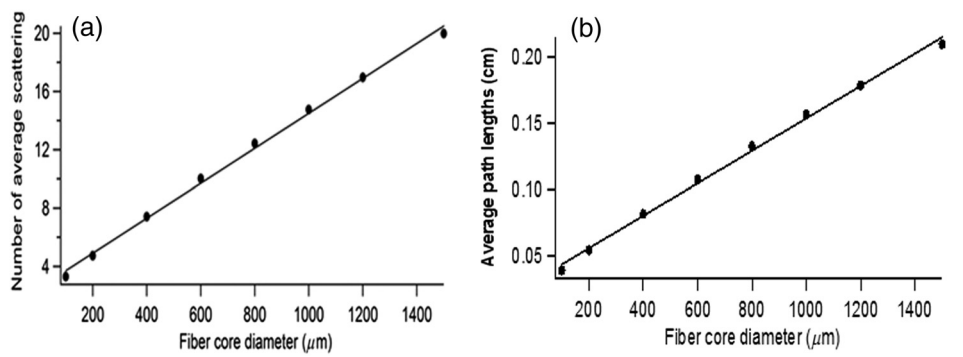

Fig. 7 (a) The average number of interactions of the collected photons by the single-fiber optical probes increases linearly with the diameter of the fibers. (b) The average path length of the collected photons increases linearly with the diameter of the fibers.

different.[20] More specifically, the wavelength dependency of the scattering anisotropy factor g and reduced scattering coefficient μ_s' for cancerous and noncancerous prostate tissues is opposite. The scattering anisotropy factor increases with wavelength for noncancerous tissue and decreases for cancerous prostate tissues in the wavelength range of 740 to 860 nm. This may be the reason for having positive and negative spectral slopes for noncancerous and cancerous prostate tissues, if the light is detected in the ballistic scattering regime. Larger spectral slopes for noncancerous tissues than for cancerous tissues may be explained by the different wavelength dependencies of the optical properties of cancerous and noncancerous tissues.[20]

5 Conclusions

Our results demonstrate that single-fiber optical probes with a diameter equal or smaller than 400 μm may be used to differentiate cancerous from noncancerous tissues, based on the sign of the spectral slopes in the wavelength range of 450 to 750 nm.

Acknowledgments

This work was supported by Akdeniz University Scientific Research Units, Antalya, Turkey.

References

1. T. P. Moffit and S. A. Prahl, "Sized-fiber reflectometry for measuring local optical properties," *IEEE J. Sel. Top. Quantum Electron.* **7**(6), 952–958 (2001).
2. F. van Leeuwen-van Zaane et al., "In vivo quantification of the scattering properties of tissue using multi-diameter single fiber reflectance spectroscopy," *Biomed. Opt. Express* **4**(5), 696–708 (2013).
3. X. W. Zhong, X. Wen, and D. Zhu, "Lookup-table-based inverse model for human skin reflectance spectroscopy: two-layered Monte Carlo simulations and experiments," *Opt. Express* **22**(2), 1852–1864 (2014).
4. X. Wen et al., "A Monte Carlo based lookup table for spectrum analysis of turbid media in the reflectance probe regime," *Quantum Electron.* **44**(7), 641–645 (2014).
5. L. T. Perelman et al., "Observation of periodic fine structure in reflectance from biological tissue: a new technique for measuring nuclear size distribution," *Phys. Rev. Lett.* **80**(3), 627–630 (1998).
6. V. Backman et al., "Polarized light scattering spectroscopy for quantitative measurement of epithelial cellular structures in situ," *IEEE J. Sel. Top. Quantum Electron.* **5**(4), 1019–1026 (1999).
7. T. P. Moffitt and S. A. Prahl, "In vivo sized-fiber spectroscopy," *Proc. SPIE* **3917**, 225–231 (2000).
8. M. Kinnunen and A. Karmenyan, "Overview of single-cell elastic light scattering techniques," *J. Biomed. Opt.* **20**, 051040 (2015).
9. M. Canpolat and J. R. Mourant, "Particle size analysis of turbid media with a single optical fiber in contact with the medium to deliver and detect white light," *Appl. Opt.* **40**(22), 3792–3799 (2001).
10. A. Amelink et al., "Single-scattering spectroscopy for the endoscopic analysis of particle size in superficial layers of turbid media," *Appl. Opt.* **42**(19), 4095–4101 (2003).
11. J. R. Mourant et al., "Mechanisms of light scattering from biological cells relevant to noninvasive optical-tissue diagnostics," *Appl. Opt.* **37**(16), 3586–3593 (1998).
12. M. Canpolat et al., "Differentiation of melanoma from non-cancerous tissue in an animal model using elastic light single-scattering spectroscopy," *Technol. Cancer Res. Treat.* **7**(3), 235–240 (2008).
13. M. Canpolat et al., "Intra-operative brain tumor detection using elastic light single-scattering spectroscopy: a feasibility study," *J. Biomed. Opt.* **14**, 054021 (2009).
14. M. Canpolat et al., "Detecting skin malignancy using elastic light scattering spectroscopy," *Proc. SPIE* **6628**, 66280K (2007).
15. M. Canpolat et al., "Elastic light single-scattering spectroscopy for detection of dysplastic tissues," *Proc. SPIE* **9032**, 90320S (2013).
16. M. Canpolat et al., "Diagnosis and demarcation of skin malignancy using elastic light single-scattering spectroscopy: a pilot study," *Dermatol. Surg.* **38**(2), 215–223 (2012).
17. J. L. Sandell and T. C. Zhu, "A review of in-vivo optical properties of human tissues and its impact on PDT," *J. Biophotonics* **4**(11–12), 773–787 (2011).
18. M. Canpolat and J. R. Mourant, "High-angle scattering events strongly affect light collection in clinically relevant measurement geometries for light transport through tissue," *Phys. Med. Biol.* **45**(5), 1127–1140 (2000).
19. J. Ramachandran et al., "Light scattering and microarchitectural differences between tumotigenic and non-tumorigenic cell models of tissue," *Opt. Express* **15**(7), 4039–4053 (2007).
20. Y. Pu et al., "Determination of optical coefficients and fractal dimensional parameters of cancerous and normal prostate tissues," *Appl. Spectrosc.* **66**(7), 828–834 (2012)

Aslinur Sircan-Kuçuksayan is a PhD student in the Department of Biophysics, Faculty of Medicine, Akdeniz University. Her research interest is tissue spectroscopy.

Tuba Denkceken received her PhD from Akdeniz University in 2014. She works as an assistant professor in the Department of Biophysics of Sanko University. Her research interest is tissue spectroscopy.

Murat Canpolat received his PhD from Istanbul Technical University in 1996. He conducted postdoctoral research at Boston University and at the Bioscience Division of Los Alamos National Laboratory, New Mexico, and worked as a research scientist at Imaging Diagnostic Systems, Inc., Florida. Since 2005, he has worked at Akdeniz University, where he is now a professor in the Department of Biophysics. His research interests include tissue spectroscopy, noninvasive cancer diagnosis, and backreflection diffuse optical tomography.